

# Fracture energy of gels

Yoshimi Tanaka<sup>1</sup>, Koji Fukao<sup>2</sup>, and Yoshihisa Miyamoto<sup>2</sup>

<sup>1</sup> Department of Mechanical Systems Engineering, Faculty of Engineering, Toyama Prefectural University, Kosugi-machi, Toyama 939-0398, Japan

<sup>2</sup> Department of Fundamental Sciences, Faculty of Integrated Human Studies, Kyoto University, Kyoto 606-8501, Japan

Received: date / Revised version: date

**Abstract.** To clarify effects of crack speed and cross-link density on fracture energy of acrylamide gels, we evaluated the roughness of the fracture surface and measured the fracture energy taking into account the roughness. The fracture energy increases linearly with crack speed  $V$  in a fast crack speed region, and the increasing rate of fracture energy with  $V$  decreases with increasing cross-link density in the gels. In a slow crack speed region the fracture energy depends on crack speed more strongly than in the fast crack speed region. This indicates that a qualitative change exists in fracture process of the gels.

**PACS.** 61.41.+e Polymers, elastomers, and plastics – 62.20.Mk Fatigue, brittleness, fracture, and cracks – 83.10.Nn Polymer dynamics

## 1 Introduction

Fracture is an old subject in material science. However, it is still extensively studied from the viewpoint both of macroscopic mechanics (fracture mechanics) and of molecular scale physics. One of the recent topics in macroscopic studies is an instability of fast cracks. Experiments [1] and simulations [2] show that the steady state propagation of a straight crack becomes unstable at a critical crack speed of the order of the Rayleigh speed in the material and accordingly roughening and branching of the crack path occur. It is believed that the instability can be essentially caused by the qualitative change of the stress field which occurs as crack speed approaches to the speed of surface wave [3,4]. On the other hand, molecular scale processes in vicinity of the crack front can also be responsible for macroscopic behavior of fracture. For example some metals undergo the so-called brittle-ductile transition. This transition is attributed to temperature dependence of mobility of dislocations emitted on the crack front [5]. Effects of molecular scale process are quite different depending on the system in question and thus the unified understanding of fracture is difficult even in the phenomenological level.

Systems classified in soft matter often show elastic or viscoelastic nature under normal conditions, and they undergo fracture with well-defined crack front lines. Fracture in the soft matter is interesting in the following two aspects. Firstly their structural units have large spatial sizes and show slow response against external forces. Thus molecular process near crack fronts can drastically change in slow fracture, which is experimentally controllable. Secondly bulk behavior of the materials against external forces deviates from the linear elasticity. To describe the fracture

phenomena of the soft matter, we should extend usual linear fracture mechanics according to physical nature of the system in question, for example, elastic large deformability of rubbers [6,7], bulk viscoelastic effect of polymer melt [8] and the anisotropic elastic energy of smectics [9].

Polymer gels [10] are one of the typical systems of the soft matter. Various phenomena in gels such as gelation, deformation and phase transition have been extensively studied. Nevertheless, few studies have been carried out on fracture of gels [11,12,13]. This is partially because gels have less industrial significance than hard solids do from the viewpoint of strength. However, in the field of polymer physics, this topic is interesting because we have much knowledge on fracture processes in other polymer systems [14] and on the various physical properties of polymer gels [15], which may be useful as a reference frame to study fracture of gels. For example, Gent and co-workers [16] showed that the strength of the butadiene rubber and that of chemically-bonded interfaces between the rubbers decrease with increasing cross-link density of the rubber. de Gennes [17] interpreted the effects as a consequence of friction during chain pulling-out process on the crack front. In gels the friction should be very small because they contain large amounts of solvent, and it is not clear whether the frictional dissipation is a dominant factor or not. The existence of solvent causes other unique effects, such as the coupling between deformation of polymer network and chemical potential of solvent. To understand fracture of gels, we should first know experimental results which show fundamental features of the phenomena.

In this study we investigate dependence of fracture energy of acrylamide gel on crack speed  $V$  and on cross-

link density in order to get the fundamental experimental results. Generally the fracture energy is determined by microscopic process near crack fronts and appears in macroscopic descriptions of fracture as an important parameter. Thus, the fracture energy is an essential physical quantity to understand the nature of fracture in gels. However, it is difficult to apply usual techniques for measuring fracture energy of hard solids to gels because of their extreme softness and large deformability. We have developed a novel method suitable for measuring fracture energy of gels and precisely measured the fracture energy of four kinds of acrylamide gel with different cross-link densities. In our method, we have adopted a peel test-like geometry to drive fracture steadily and taken account of roughness of fracture surfaces to evaluate the fracture energy of the gels. Following results are obtained. (i) For each cross-link density, the fracture energy is an increasing function of  $V$  and when we change  $V$ , a crossover occurs; in the faster  $V$  side of the crossover the fracture energy linearly increases with  $V$  and in the slower  $V$  side, where roughening of the fracture surfaces is remarkable and the correction about the area of the fracture surfaces played an important role, the fracture energy depends on  $V$  with larger increasing rate than in the faster  $V$  side. (ii) At a given value of  $V$ , both the value of fracture energy and the increasing rate of the fracture energy with  $V$  decrease with increasing the cross-link density.

## 2 Experiment

*Samples*— We use as samples four kinds of acrylamide gels which have same polymer concentration and different cross-link densities. The amount of each reagent for preparing acrylamide gels is shown in Table 1. Acrylamide monomer (AA,  $M_w = 71.08$ ) constitutes sub-chains and methylenebisacrylamide (BIS,  $M_w = 154.17$ ) constitutes cross-links. Ammonium persulphate (APS) is an initiator and tetramethylethylenediamine (TEMED) is an accelerator of the radical polymerization of AA and BIS. We will distinguish the samples by the codes of 4BIS ~ 10BIS as shown in Table 1. To make pillar-shaped gels (2cm×1.8cm×14cm), pre-gel solutions produced according to Table 1 were poured into containers in which molds were arranged and left for 24 hours at 25 °C. The gels are took off from the molds and used for the fracture experiment. The values of Young's modulus  $E$  and velocity of transverse wave of the gels  $V_t$  are also shown in Table 1. The values of  $E$  are measured by compressing the gels.

To calculate  $V_t$  we used the value of density  $\rho = 1.01$  (g/cm<sup>3</sup>), and the value of Poisson's ratio  $\nu = 1/2$ .

*Peel test like method*— In order to measure the fracture energy of the gel we developed a method which is similar to the peel test. In Fig. 1 we present a gel fractured by the method. The set-up of the experiment is as follows. We put the pillar-shaped gel on an aluminum plate and heated the aluminum plate with a gas burner for about ten seconds. By this treatment the sample gel is fixed on the aluminum plate. We attached a strip of a filter paper to the upper surface of the gel. The filter paper is tightly absorbed to the gel. We created an initial notch on one of the smallest surface of the gel and made it propagate by 2cm by pulling the filter paper with hands. An end of the filter paper was connected to a stepping motor located well above the gel (1.8m) through a strain-gauge and a wire. A thin layer of the gel (~1mm) is peeled off by rolling up the wire with the stepping motor. The control parameter is the rolling speed  $V$  which is equal to the crack speed  $V$  in our 90° peeling geometry. The measured quantity is the peeling force  $F(t)$ .

*Fracture energy*— Fracture energy  $G$  is defined as the energy needed to make a unit area of a fracture surface. In our peel-test like method the fracture energy  $G$  is calculated by the following equation,

$$G = \frac{F}{w} \quad (1)$$

where  $F$  is the measured force and  $w$  is the width of the pillar-shaped gel (see Fig. 1). In order to understand this relation, let us suppose that the crack front in Fig. 1 steadily propagates over a distance  $\Delta x$  along the direction of the longest axis. The increase in area of the fracture surface by this propagation of the crack front is  $w \times \Delta x$  and the energy required to extend the fracture surface is the work done to the gel,  $F \times \Delta x$ . Therefore the fracture energy  $G$  is  $(F \times \Delta x)/(w \times \Delta x)$ . This is identical to the quantity mentioned above.

*Roughness of fracture surfaces*— In this study we evaluate the roughness of the fracture surfaces using replicas produced by molding the fracture surfaces using silicon rubber. The replica was cut along the plane which was normal to the global fracture surface and parallel to the direction of fracture propagation. The shape of the cross section was recorded by an image scanner (Microtek, Scan-Maker III). A quantity which can be regarded as a measure of the roughness of the fracture surfaces was extracted from the image of the cross section.

Sample code	Water	AA	BIS	APS	TEMED	$E(\text{dyn/cm}^2)$	$V_t(\text{cm/s})$
4BIS	100cc	10g	0.04g	0.1g	0.25cc	$0.56 \times 10^5$	135
6BIS	100cc	10g	0.06g	0.1g	0.25cc	$1.21 \times 10^5$	200
8BIS	100cc	10g	0.08g	0.1g	0.25cc	$1.86 \times 10^5$	248
10BIS	100cc	10g	0.10g	0.1g	0.25cc	$2.77 \times 10^5$	302

**Table 1.** The composition of each reagent required to prepare the four kinds of acrylamide gels, Young's modulus  $E$  and velocity of transverse wave  $V_t$  of the gels.

### 3 Results

Figure 2a is  $F(t)$  at  $V = 0.4 \text{ cm/s}$ . The arrows indicate the initiation and the termination of the fracture propagation. The fracture propagates steadily in the period of time between the arrows. We divided the period of time corresponding to the steady state fracture propagation equally into three periods and evaluated the fracture energy  $G$  using the time average of  $F(t)$  for the central period.

Figure 2b is  $F(t)$  at  $V = 0.04 \text{ cm/s}$ . As shown in Fig. 2a there is a period of time corresponding to a steady state fracture propagation. However the fluctuation of  $F(t)$  in Fig. 2b is larger than that in Fig. 2a even in the period of the steady state fracture propagation. The increase in fluctuation of  $F(t)$  is characteristic of slow fracture and is accompanied with roughening of fracture surfaces. We show evidence for the existence of the roughening of fracture surface later (see Fig. 5 and Fig. 6).

Figure 3 is a plot of the fracture energy  $G$  as a function of crack speed  $V$ . At fast values of  $V$  ( $V > 1 \text{ cm/s}$ ),  $G(V)$  depends linearly on  $V$  and both  $G(V)$  and  $dG/dV$  decrease with increasing BIS concentration of the samples. Figure 4 is a plot of the fracture energy  $G(V)$  of 4BIS, 6BIS and 8BIS for  $V < 1 \text{ cm/s}$ . A common feature of  $G(V)$  for these samples is that there is a region of  $V$  where  $G$  increases with decreasing  $V$ , and  $G(V)$  has a minimum (shown by the upward arrows in Fig. 4) at a value of  $V$ . Hereafter, we will call this  $V_{min}$ . The dependence of  $G(V)$  on BIS concentration is non-monotonical below the value of  $V \cong 0.8 \text{ cm/s}$ .

As  $V$  decreases across  $V_{min}$ , the roughness of the fracture surfaces grows up (the roughening at *slow fracture*). In Figures 5a-c we show the morphologies of fracture surface of 6BIS at different crack speeds. The bars represent  $0.9 \text{ cm}$ . Figures 5e-g show the cross sections of the fracture surfaces shown in Figs. 5a-c, respectively. The cross section is along the plane which is perpendicular to the global fracture surfaces and contains the center lines of the fracture surfaces (the  $x$ -axis in Fig. 5d). The vertical size of the cross section corresponds to  $3 \text{ cm}$  and the horizontal size is magnified 2.5 times compared with the true scale. The shape of right-hand side boundary of the cross-section corresponds to the  $h(x)$  shown in the illustration, i.e., the height of the fracture surface measured at each point of the  $x$ -axis. Figure 5a is a fracture surface of 6BIS above  $V_{min}$ . At such crack speeds most parts of fracture surface are flat and a few steps exist on the global fracture surface which seem like lines in Fig. 5a. Around  $V_{min}$ , such steps are frequently produced and the roughness of the fracture surfaces begins to grow up (Fig. 5b). As  $V$  decreases further, the roughness of the fracture surfaces becomes more remarkable (Fig. 5c).

To quantify the roughness of the fracture surfaces we introduce a quantity  $R$  defined by the following equations.

$$R \equiv \frac{\int_{l_c} \sqrt{1 + (dh/dx)^2} dx}{\int_{l_c} dx} \quad (2)$$

$$= \left\langle \sqrt{1 + (dh/dx)^2} \right\rangle,$$

where the range of integration  $l_c$  represents the distance along the  $x$ -axis which corresponds to the central period of time in which the average of  $F(t)$  is took (see the first paragraph of this section), and the symbol  $\langle \dots \rangle$  represents the spatial average over the distance. The numerator on right-hand side in (2) is the contour length of  $h(x)$  over the distance, thus  $R$  is equal to 1 for the completely flat fracture surface ( $dh/dx = 0$ ) and increases from 1 as the roughness of the fracture surface increases. Therefore,  $R$  is an index of the roughness of the fracture surfaces.

In Fig. 6 we show  $R$  as a function of the crack speed  $V$  for four kinds of sample gels.  $R(V)$  of the gels has a common feature; i.e. at fast values of  $V$ ,  $R$  is close to 1 and with decreasing  $V$ ,  $R$  begins to increase at the value of  $V$  close to  $V_{min}$ . This fact clearly shows the correlation between the roughening of fracture surfaces and the increase in  $G(V)$  with decreasing  $V$  across  $V_{min}$ .

When we take into account the roughness of fracture surfaces, we should correct the fracture energy by dividing it by  $R^2$ . Strictly speaking, we should measure the same quantity as  $R$  along the lateral direction in Fig. 5,  $R'$ , and divide  $G(V)$  by  $RR'$ . However, the structures causing the roughening are the steps on the fracture surfaces extending at  $45^\circ$  from the  $x$ -axis. Therefore we can expect  $R$  and  $R'$  are very close. In Fig. 7 and Fig. 8, we show the corrected fracture energy  $\bar{G}(V) \equiv G(V)/R(V)^2$ . Behavior of  $\bar{G}(V)$  at fast values of  $V$  is qualitatively identical to that of  $G(V)$ , i.e.,  $\bar{G}(V)$  linearly increases with  $V$  and  $\bar{G}(V)$  and  $d\bar{G}/dV$  decrease with BIS concentration. On the other hand, when  $V$  decreases, the crossover in  $\bar{G}(V)$  occurs in the narrow range of  $V$ , and below the crossover range  $d\bar{G}/dV$  becomes larger than above the crossover range. As a result of the correction,  $\bar{G}(V)$  at each value of  $V$  in the region monotonically depends on BIS concentration as in the fast  $V$  region.

Our results for the corrected fracture energy  $\bar{G}$  can be summarized as follows:

- i) At a given value of  $V$ ,  $\bar{G}(V)$  decreases with increasing BIS concentration.
- ii) At fast values of  $V$  ( $V > 1 \text{ cm/s}$ ),  $\bar{G}(V)$  for each BIS concentration linearly increases with  $V$ .
- iii) The increasing rate  $d\bar{G}/dV$  decreases with increasing BIS concentration.
- iv) With decreasing  $V$  across a crossover range,  $d\bar{G}/dV$  becomes larger.

### 4 Discussion

In the first half of this section we will discuss the corrected fracture energy  $\bar{G}$ . As shown in Figs. 7-8, the order of the fracture energy  $\bar{G}(V)$  of the gels is several hundred times as large as that of the surface tension of water (about  $72 \text{ dyn/cm}$  at  $25^\circ\text{C}$  [18]). Thus  $\bar{G}(V)$  reflects energy needed for breaking the network structure of the gels near crack fronts and consists of two parts; one is due to cutting polymer chains of the gel network  $G_{cut}$ , the other is due to viscous resistance  $G_{vis}$ .

$$\bar{G} = G_{cut} + G_{vis}. \quad (3)$$

Gels synthesized from monomer solutions contain various kinds of defects. Characterization of the gels is open problems in polymer physics; We can not give quantitative discussions about our results from the microscopic viewpoint. However, the elastic modulus of the gels used in this study increases with BIS concentration as shown in Table 1. This shows that actual cross-link density increases with BIS concentration. The following qualitative discussion can be made on  $\bar{G}(V)$ .

We first consider the number of polymer chains cut on the fracture surface of the gels. If all cross-linkings of a gel disappear, the system would be a solution of linear polymer, and we could divide it into two pieces without cutting any polymer chain. On the threshold cross-link density of gelation, we need cut a finite number of the polymer chains. With increasing the cross-linking density, we need to cut more number of the polymer chains on the fracture surfaces. From this consideration, we expect that  $G_{cut}$  increases with BIS concentration.

We next consider the number of elements which cause viscous resistance for extension of a fracture surface. Dangling chains, which have free ends, should be such structures. Another possibility is the sub-chains long enough to penetrate into other part of the gel. As the cross-linking density decreases, i.e., as network structure of gels becomes looser, the number of the elements increases. Thus, we can expect that  $G_{vis}$  increases with decreasing the BIS concentration.

From above consideration, we can conclude that the result i) shows  $G_{vis}$  overwhelms  $G_{cut}$  at the values of  $V$  accessed in this study. The result ii) shows that  $G_{vis}$  can be represented by the following form,

$$G_{vis} = \alpha V. \quad (4)$$

The result iii) shows that the prefactor  $\alpha$  decreases with increasing the BIS concentration. This is reasonable because  $\alpha$  should be an increasing function of the number of the elements contributing to viscous resistance.

The physical meaning of iv) becomes clear if we exchange the ordinate and the abscissa of Fig. 7 and we recall that  $\bar{G}$  is proportional to the force driving the fracture. Above a critical value of  $V$ , an increase of the driving force  $\bar{G}$  causes larger increase of  $V$  than below the critical value. This type of nonlinear relation between a driving force and the conjugate rate is often observed in soft polymeric systems; for example, the relation in stress/strain rate of polymer melts (shear thinning) [19] and the relation in loading/detaching speed of glass-rubber interfaces stitched by linear polymers [20], etc. In essence these phenomena are explained by conformational change of polymers due to the driving force [21]. This mechanism may be applicable to fracture of gels.

At present, we do not identify the origin of  $G_{vis}$ . A possibility is the bulk viscoelastic dissipation. Moreover, strong nonlinear process localized near crack fronts, for example, chain pulling-out, may participate in  $G_{vis}$ . To clarify this point, we need another experiment where we use more controlled gels.

Now we discuss the phenomena related to the roughening of fracture surfaces. As shown in Figs. 4-6, the ap-

parent fracture energy  $G(V)$  increases with decreasing  $V$ , accompanied with the roughening of the fracture surfaces. This means that fracture of the gels does not follow the path of minimum dissipation. In other words, under slow fracture conditions gels increase their strength by undulating crack front lines. On phenomenological level, similar  $V$ - $G$  curve is reported in fracture of glassy polymers such as PMMA [14,22], which is attributed to crazing. The crazing, which is a kind of plastic deformation, is characteristic of glassy polymers, and we can not expect concrete relation in molecular level between the  $V$ - $G$  curve of gels and that of glassy polymers.

Scale invariant nature of rough fracture surfaces is one of the topics in physical study of fracture. Theoretically, it has been studied as a stochastic effect [23]. In the gels, the roughening is caused by the definite elements, i.e., steps on fracture surfaces extending to the direction of  $\pm 45^\circ$  from the  $x$ -direction.<sup>1</sup> (In a previous work [13] we clarified the structures on crack fronts which create the oblique step-lines, and classified collision process between the structures.) This result gives a new viewpoint on the general study for the rough fracture surfaces.

Wallner [24] reported similar oblique step-lines on fracture surfaces on glass (Wallner lines). The proposed mechanism [25] is that the Wallner lines are created at the parts of a moving crack front where stress field is disturbed by stress pulses which are nucleated when the crack front passed through irregular points of the material, i.e., the Wallner lines are loci of the intersections between the crack front and fronts of stress pulses. This mechanism does not hold for the step-lines of gels because the  $\pm 45^\circ$  oblique step-lines of gels are observed even at much slower values of  $V$  than the sound velocity in the gels; in fracture process in Fig. 5c, for example, the crack front ( $V = 0.015\text{cm/s}$ ) is almost stationary compared with the stress pulses ( $V_t = 200\text{cm/s}$ , see Table 1), and the loci of the intersections are almost along the crack front itself, i.e., almost horizontal in Fig. 5c. This does not agree with the  $\pm 45^\circ$  obliquity of the step-lines. On the other hand, with regard to geometrical aspect it is probable that the Wallner lines are created by similar structure on crack fronts to that observed in gels.

<sup>1</sup> Besides the oblique step-lines, scratch-like steps extending along the  $x$ -direction can be seen in Figs. 5a-c. From qualitative observation by eyes and by low magnification microscope, following tendency is recognized: (i) Large(thick) steps are the oblique type and small(thin) steps are the scratch-like type. (ii) the critical height of steps becomes larger as  $V$  increases. Two kinds of morphological transition occur on fracture surfaces of gels: One is the roughening transition which is related to nucleation frequency of the steps on the whole of a crack front, the other is the oblique/scratch-like transition of each step-line. In a previous study [12] where we used acrylamide gels of higher polymer concentration and lower cross-link density than those used in the present study, we confused these two transitions because in the gel used in the previous study the coexistence of the two kinds of steps occurs only in relatively narrow range of  $V$  ( $V \sim 0.5\text{ cm/s}$ ) and the roughening transition occurs in the same range. We will report on details of the morphological transition elsewhere.

In summery, we studied dependence of the fracture energy on the crack speed  $V$  and on cross-link density, taking account of the roughness of the fracture surfaces. The following features is found on  $V$  dependence of the fracture energy; (i) At a given value of  $V$ , the fracture energy decreases with the cross-link density. (ii) At fast values of  $V$  ( $V > 1\text{cm/s}$ ), the fracture energy linearly increases with  $V$ , and at slow values of  $V$  the fracture energy increases with  $V$  with larger increasing rate than at fast values of  $V$ . These results indicate that the dissipative effects dominate over the effects of the breakage of polymer chains in the fracture of gels.

The authors thank Professor Ken Sekimoto for conducting us to study of this field. They also thank to Professor Fumihiko Tanaka and Professor Mitsugu Matsushita for their helpful comments. This work was partly supported by a Grant-in-Aid from the Ministry of Education, Science, Sports and Culture of Japan.

## References

1. J. Fineberg, S. P. Gross, M. Marder and H. L. Swinney, Phys. Rev. B **45**, 5146(1993).
2. F. F. Abraham, D. Brodbeck, R. A. Rafey, W. E. Rudge, Phys. Rev. Lett **73**, 2336(1994).
3. E. S. C. Ching, H. Nakanishi and J. S. Langer, Phys. Rev. B **45**, 1087(1996).
4. L. B. Freund, *Dynamical Fracture Mechanics*, Cambridge Univ. Press, New York, 1990.
5. F. C. Serbena and S. G. Roberts, Acta metall. Mater., **42**, 2505(1994).
6. R. S. Rivlin and A. G. Thomas, J. Polym. Sci., **10**, 291-318(1953).
7. E. H. Andrews, J. Mat. Sci., **9**, 887(1974).
8. P. G. de Gennes, *Langmuir*, **12**, 4497(1996).
9. P. G. de Gennes, *Europhys.Lett.*, **13**, 709(1990).
10. P.-G. de Gennes, *Scaling Concepts in Polymer Physics*, Cornell University Press, Ithaca, New York, 1979.
11. D. Bonn, H. Kellay, M. Prochnow, K. Ben-Djemaa and J. Meunier, Science **280**, 265(1998).
12. Y. Tanaka, K. Fukao, Y. Miyamoto, H. Nakazawa and K. Sekimoto, J. Phys. Soc. Jpn., **65**, 2349(1996).
13. Y. Tanaka, K. Fukao, Y. Miyamoto and K. Sekimoto, *Europhys.Lett.*, **43**, 664(1998).
14. A. J. Kinloch and R. J. Young, *Fracture Behavior of Polymers*, Elsevier, London and New York, 1983.
15. Y. Li and T. Tanaka, Anu. Rev. Mater. Sci. **22**, 243(1992).
16. A. N. Gent, Int. J. Adh. Adhes. April issue 175(1981).
17. P. G. de Gennes, Can. J. Phys. **68**, 1049(1990).
18. *CRC Handbook of Chemistry and Physics*, ed. R.C. Weast, Chemical Rubber Company, 1999.
19. M. Doi and S. F. Edwards, *The Theory of Polymer Dynamics*, Oxford Univ. Press, Clarendon, 1986.
20. C. Creton, H. R. Brown and K. R. Shull, Macromolecules, **27**, 3174(1994).
21. A. Ajdari, F. Brochard, P. G. de Gennes, L. Leibler, J. L. Viovy and M. Rubinstein, Physica A, **204**, 17(1994).
22. W. Döll and L. Könczöl, in *Advances in Polymer Science* (Vol. 91/92), eds. H. H. Kausch, Springer, Berlin, 1990.
23. J. P. Bouchaud, E. Bouchaud, G. Lapasset and J. Planès, Phys. Rev. Lett. **71**, 2240(1993).
24. V. H. Wallner and H. a. d. Saale, Z. Physik, **114**, 368(1939).
25. D. G. Holloway, *The Physical Properties of Glass*, Wykeham Pub., London, 1973.

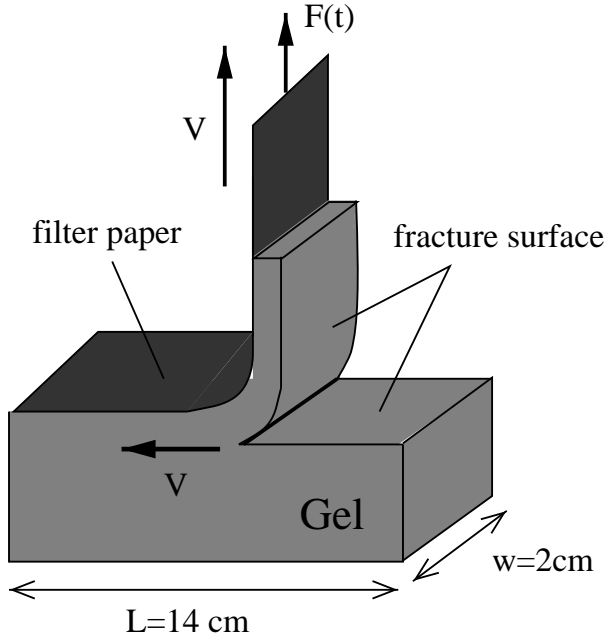


**Fig. 1.** A schematic of a gel undergoing fracture. We fixed the gel on the aluminum plate and made an initial notch and attached the filter paper to the upper surface. By pulling-up the filter paper vertically at a constant speed  $V$ , the crack propagates through the gel at the rate  $V$ . The force needed in pulling-up  $F(t)$  is measured with a strain-gauge.

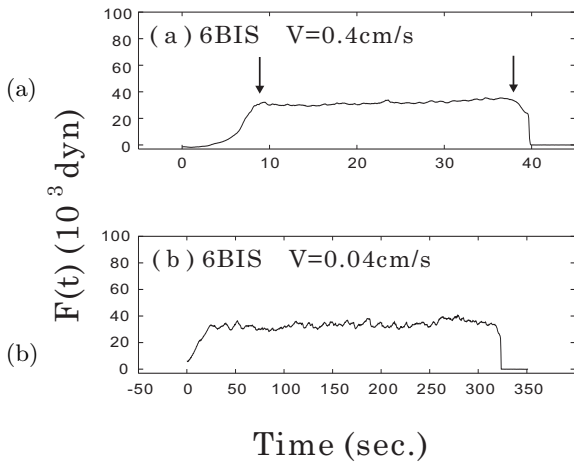


**Fig. 2.** Examples of measured peeling force  $F(t)$ . (a) is an example of  $F(t)$  at  $V = 0.4 \text{ cm/s}$ . The arrows indicate the initiation and the termination of fracture. In the period of time between the arrows, the fracture steadily propagated. The fracture energy  $G$  was evaluated from the averages of  $F(t)$  in the central part of the period. (b) is an example of  $F(t)$  at  $V = 0.04 \text{ cm/s}$ . Fluctuation of  $F(t)$  is larger compared with (a).

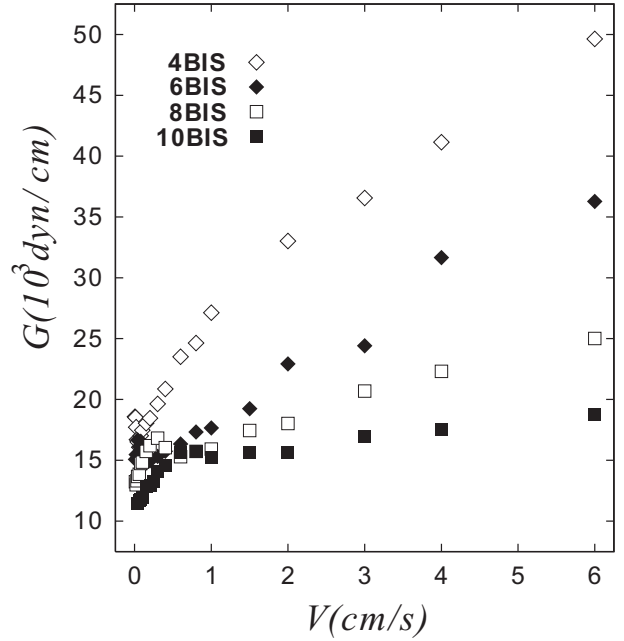


**Fig. 3.** The fracture energy  $G(V)$ . At fast values of  $V$  ( $V > 1 \text{ cm/s}$ ),  $G(V)$  of each sample linearly increases with  $V$ . In the region,  $G$  at a given value of  $V$  decreases with the BIS concentration. At slow values of  $V$ ,  $G$  depends on  $V$  in more complex fashion.

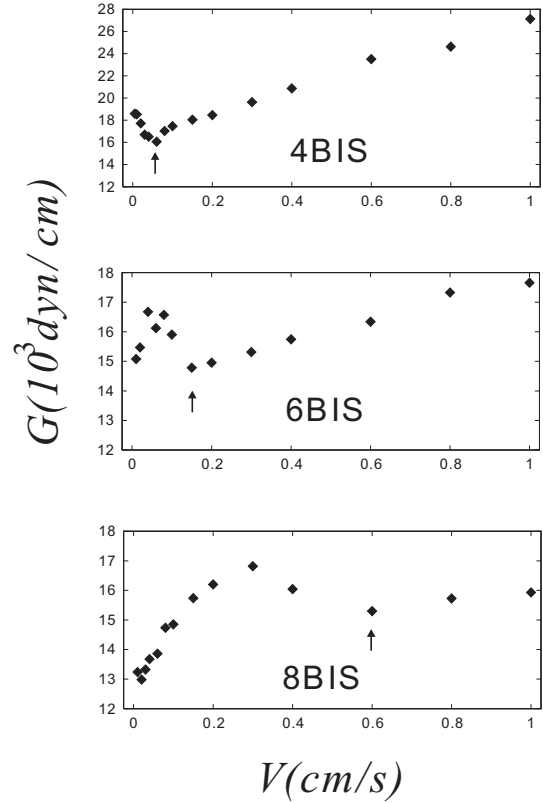


**Fig. 4.**  $G(V)$  of 4BIS, 6BIS and 8BIS for  $V < 1 \text{ cm/s}$ .  $G(V)$  non-monotonically depends on  $V$  in the region and the minimum of  $G(V)$  exists.

See attached jpg file (fig5.jpg) !

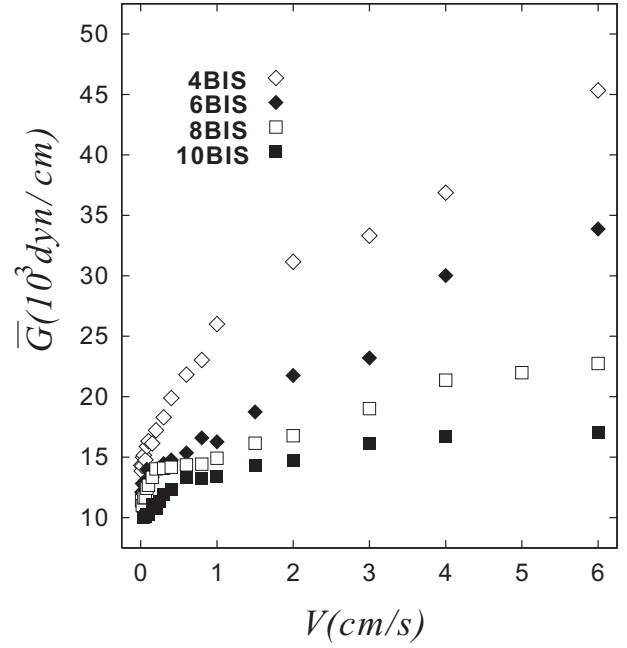


**Fig. 5.** (a)-(c): Examples of the fracture surfaces of 6BIS. The fracture propagated from top to bottom of each figure. The bars represent 0.9 cm. (d): An illustration of a fracture surface in which the  $x$ -axis and the profile of the height of fracture surfaces  $h(x)$  are defined. (e)-(g): cross sections of the fracture surfaces shown in (a)-(c), respectively. Shapes of the right-hand side boundaries of (e)-(g) represent  $h(x)$ .

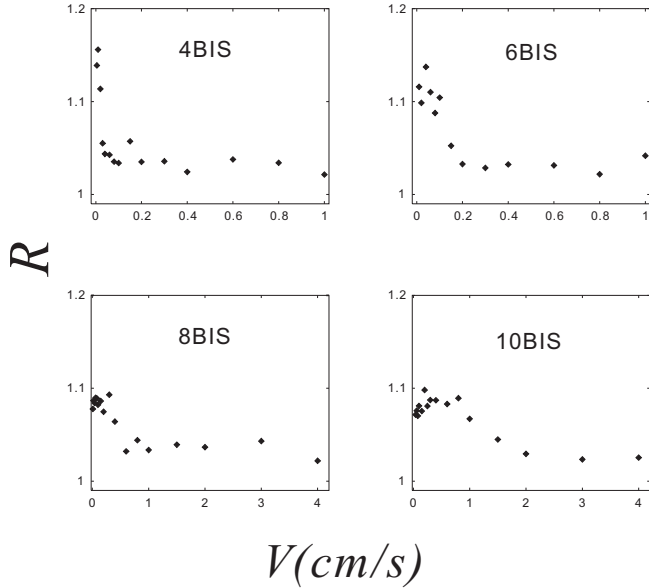


**Fig. 6.** An index of the roughness  $R \equiv \langle \sqrt{1 + (dh/dx)^2} \rangle$  as a function of  $V$ . As  $V$  decreases,  $R$  begins to grow up. The value of  $V$  at which the  $R$  begin to grow up (indicated in Fig. 4 by upward arrows) corresponds to the value of  $V$  which gives the minimum of  $G(V)$  in Fig. 4.

**Fig. 7.** The corrected fracture energy  $\bar{G}(V) \equiv G(V)/R(V)^2$ . At fast values of  $V$ , behavior of  $\bar{G}(V)$  is qualitatively identical to that of  $G(V)$ .

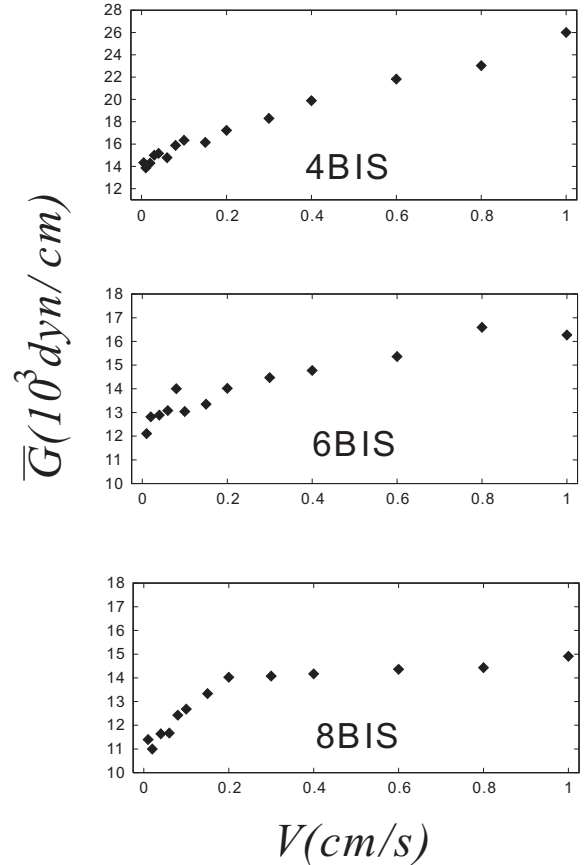


**Fig. 8.**  $\bar{G}(V)$  of 4BIS, 6BIS and 8BIS for  $V < 1$  cm/s. In this region  $\bar{G}(V)$  monotonically depends on  $V$ . This is quite different from the behavior of  $G(V)$  in Fig. 4.

This figure "fig5.jpg" is available in "jpg" format from:

<http://arXiv.org/ps/cond-mat/0003474v2>